

Using a Decoupling Technique to Identify the Magnetic Flux in a Permanent Magnet Synchronous Motor

Paolo Mercorelli

Abstract—Unknown parameters cause difficulties in the control of permanent magnetic motors. Particular techniques are requested to be able to achieve an appropriately controlled dynamics identification. A geometric approach for achieving a decoupling of the system is applied in the presented strategy. The decoupling makes the estimation of the Permanent Magnet Synchronous Motor (PMSM) parameters easier. A feedback controller in combination with the feed-forward controller being generated by an input partition, achieves the decoupling. This can be applied to various types of motors or systems in case of the decoupling conditions being satisfied. A control together with the identification method is tested in the simulation section. The presented simulation and measured results are shown for validation of the strategy which is proposed.

Index Terms—Permanent Magnet Synchronous Motor, Identification, PWM control

I. INTRODUCTION AND MOTIVATIONS

Recently the interest in the topic of geometric control has increased in theoretical aspects and applications as well, see for instance [1], particularly in control problems like Non-interaction and Model Predictive Control, see [2]. It is known that, an accurate knowledge of the model and its parameters is necessary for realising an effective control. For achieving a desired system performance, advanced control systems are usually required to provide fast and accurate response, quick disturbance recovery and parameter variations insensitivity [3]. Acquiring accurate models for systems under investigation is usually the fundamental part in advanced control system designs, see [4]. In [4] a Permanent Magnet Synchronous Motor (PMSM) is considered with a PI controller. A chopper strategy is proposed and a parameter set up of the above mentioned PI-regulator is proposed to obtain a smooth tracking dynamics even though a chopper control structure is included in the drive. High performance application of permanent magnet synchronous motors (PMSM) is increasing. In particular, application in electrical vehicles is very much used. The existing applications chopper control structures are very popular because they are very cheap and easy to be realised. Nevertheless, using a chopper control structure smooth tracking dynamics could be difficult to obtain without increasing the switching frequency because of the discontinuity of the control signals. No smooth tracking dynamics lead to a not comfortable travel effect for the passengers of the electrical vehicle.

Paolo Mercorelli is with the Institute of Product and Process Innovation, Leuphana University of Lueneburg, Volgershall 1, D-21339 Lueneburg, Germany Tel.: +49-(0)4131-677-5571, Fax: +49-(0)4131-677-5300. mercorelli@uni.leuphana.de.

PMSMs as traction motors are common in electric or hybrid road vehicles and their importance will increase in the future because of the dissemination of electrical mobility. Moreover, in electrical mobility the control strategies, connected with an optimal energy management, represent a decisive point for the success of effective technologies and products, [5]. PMSMs have, in terms of control, already consolidated methods and techniques. For rail vehicles, PMSMs as traction motors are not widely used yet. Although the traction PMSM can bring many advantages, just a few prototypes of vehicles were built and tested. The next two new prototypes of rail vehicles with traction PMSMs were presented on InnoTrans fair in Berlin 2008 Alstom AGV high speed train and skoda Transportation low floor tram 15T ForCity. Advantages of PMSM are well known. The greatest advantage is low volume of the PMSM in comparison with other types of motors. It makes a direct drive of wheels possible. On the other hand, the traction drive with PMSM has to meet special requirements typical for overhead line fed vehicles.

The most common parameters required for the implementation of such advanced control algorithms are the classical simplified model parameters: L_d - the direct axis self-inductance, L_q - the quadrature axis self-inductance, and Φ - the permanent magnet flux linkage. Techniques have been proposed for the parameters' identification of a PMSM from different perspectives, such as offline [6], [7] and online identification of PMSM electrical parameters, [8]. These techniques are based on the decoupled control of linear systems when the motor's mechanical dynamics are ignored. Using a decoupling control strategy, internal dynamics may be almost obscured, but it is useful to remember that there are no limitations in the controllability and observability of the system. In the report by [9] a decoupling technique is used to control a permanent magnets machine more efficiently in a sensorless way using an observer. Despite limitations on the frequency range of identification, this paper proposes a dynamic observer based on a geometric decoupling technique to estimate parameter Φ . The proposed identification technique, similar to that presented in [10], applies a procedure based on the work in [11]. In the meantime, the paper proposes a particular observer that identifies the permanent magnet flux using the estimated L_{dq} and R_s parameters from an ARMA identification structure as presented in [11]. The paper is organised in the following way: a sketch of the model of the synchronous motor and its behaviour are given in

Section II, Section III is devoted to deriving, proposing and discussing the dynamic estimator, and Section IV shows the simulation results using real data for a three-phase PMSM.

The main nomenclature

$\mathbf{u}_{in}(t) = [u_a(t), u_b(t), u_0(t)]^T$: three phase input voltage vector
 $\mathbf{i}(t) = [i_a(t), i_b(t), i_0(t)]^T$: three phase input current vector
 $\mathbf{u}_q(t)$: induced voltage vector
 ω_{el} : electrical pulsation
 R_s : coil resistance
 L_{dq} : dq coil inductance
 \mathbf{A} : state matrix of the electrical model
 \mathbf{B} : input matrix of the electrical model
 $\mathcal{B} = \text{im}\mathbf{B}$: image of matrix \mathbf{B} (subspace spanned by the columns of matrix \mathbf{B})
 $\min\mathcal{I}(\mathbf{A}, \mathcal{B}) = \sum_{i=0}^{n-1} \mathbf{A}^i \text{im}\mathbf{B}$: minimum \mathbf{A} -invariant subspace containing $\text{im}(\mathbf{B})$
 \mathbf{F} : decoupling feedback matrix field
 $\mathbf{g}(\omega_{el})$: Park transformation
 $\mathbf{T}(\omega_{el})$: decoupling feedforward matrix field
 \mathcal{I} : invariant subspace
 \mathcal{C}_d : kernel of output matrix \mathbf{C}_d (d component of the current)
 \mathcal{C}_q : kernel of output matrix \mathbf{C}_q (q component of the current)
 \mathcal{C}_0 : kernel of output matrix \mathbf{C}_0 (0 component of the current)

II. MODEL OF A SYNCHRONOUS MOTOR

For aiding advanced controller design for PMSM, it is very important to obtain an appropriate model of the motor. A good model should not only be an accurate representation of system dynamics but it should also facilitate the application of the existing control techniques. Among a variety of models presented in the literature since the introduction of PMSM, the two-axis dq-model, obtained using Park dq-transformation is the most widely used in variable speed PMSM drive control applications [3] and [8]. The Park dq-transformation is a coordinate transformation that converts the three-phase stationary variables into variables in a rotating coordinate system. In dq-transformation, the rotating coordinate is defined relative to a stationary reference angle as illustrated in Fig. 1. The dq-model is considered in this work.

$$\begin{bmatrix} u_d(t) \\ u_q(t) \\ u_0(t) \end{bmatrix} = \begin{bmatrix} \frac{2 \sin(\omega_{el} t)}{3} & \frac{2 \sin(\omega_{el} t - 2\pi/3)}{3} & \frac{2 \sin(\omega_{el} t + 2\pi/3)}{3} \\ \frac{2 \cos(\omega_{el} t)}{3} & \frac{2 \cos(\omega_{el} t - 2\pi/3)}{3} & \frac{2 \cos(\omega_{el} t + 2\pi/3)}{3} \\ \frac{1}{3} & \frac{1}{3} & \frac{1}{3} \end{bmatrix} \begin{bmatrix} u_a(t) \\ u_b(t) \\ u_c(t) \end{bmatrix}, \quad (1)$$

$$\begin{bmatrix} i_d(t) \\ i_q(t) \\ i_0(t) \end{bmatrix} = \begin{bmatrix} \frac{2 \cos(\omega_{el} t)}{3} & \frac{2 \cos(\omega_{el} t - 2\pi/3)}{3} & \frac{2 \cos(\omega_{el} t + 2\pi/3)}{3} \\ \frac{-2 \sin(\omega_{el} t)}{3} & \frac{-2 \sin(\omega_{el} t - 2\pi/3)}{3} & \frac{-2 \sin(\omega_{el} t + 2\pi/3)}{3} \\ \frac{1}{3} & \frac{1}{3} & \frac{1}{3} \end{bmatrix} \begin{bmatrix} i_a(t) \\ i_b(t) \\ i_c(t) \end{bmatrix}. \quad (2)$$

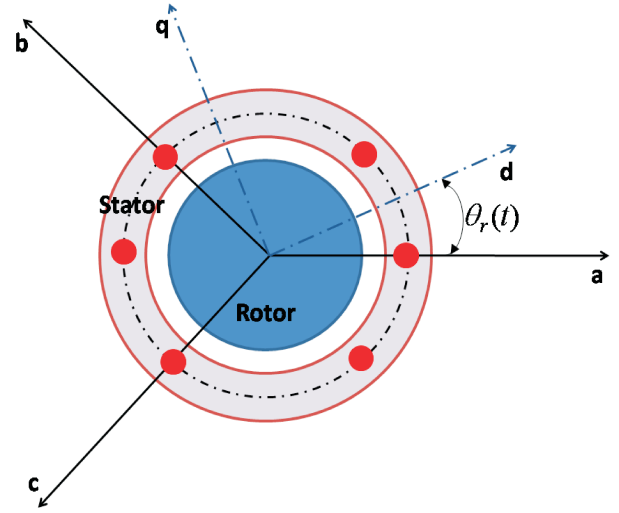


Fig. 1. Park transformation for the motor

The dynamic model of the synchronous motor in dq-coordinates can be represented as follows:

$$\begin{bmatrix} \frac{di_d(t)}{dt} \\ \frac{di_q(t)}{dt} \end{bmatrix} = \begin{bmatrix} -\frac{R_s}{L_d} & \frac{L_q}{L_d} \omega_{el}(t) \\ -\frac{R_s}{L_q} & -\frac{L_d}{L_q} \omega_{el}(t) \end{bmatrix} \begin{bmatrix} i_d(t) \\ i_q(t) \end{bmatrix} + \begin{bmatrix} \frac{1}{L_d} & 0 \\ 0 & \frac{1}{L_q} \end{bmatrix} \begin{bmatrix} u_d(t) \\ u_q(t) \end{bmatrix} - \begin{bmatrix} 0 \\ \frac{\Phi \omega_{el}(t)}{L_q} \end{bmatrix}, \quad (3)$$

and

$$M_m = \frac{3}{2} p \{ \Phi i_q(t) + (L_d - L_q) i_d(t) i_q(t) \}. \quad (4)$$

In (3) and (4), $i_d(t)$, $i_q(t)$, $u_d(t)$ and $u_q(t)$ are the dq-components of the stator currents and voltages in synchronously rotating rotor reference frame, $\omega_{el}(t)$ is the rotor electrical angular speed, the parameters R_s , L_d , L_q , Φ and p are the stator resistance, d-axis and q-axis inductance, the amplitude of the permanent magnet flux linkage, and p the number of couples of permanent magnets, respectively. At the end, M_m indicates the motor torque. Considering an isotropic motor with $L_d \simeq L_q = L_{dq}$, it follows:

$$\begin{bmatrix} \frac{di_d(t)}{dt} \\ \frac{di_q(t)}{dt} \end{bmatrix} = \begin{bmatrix} -\frac{R_s}{L_{dq}} & \omega_{el}(t) \\ -\frac{R_s}{L_{dq}} & \omega_{el}(t) \end{bmatrix} \begin{bmatrix} i_d(t) \\ i_q(t) \end{bmatrix} + \begin{bmatrix} \frac{1}{L_{dq}} & 0 \\ 0 & \frac{1}{L_{dq}} \end{bmatrix} \begin{bmatrix} u_d(t) \\ u_q(t) \end{bmatrix} - \begin{bmatrix} 0 \\ \frac{\Phi \omega_{el}(t)}{L_{dq}} \end{bmatrix}, \quad (5)$$

and

$$M_m = \frac{3}{2} p \Phi i_q(t), \quad (6)$$

with the following movement equation:

$$M_m - M_w = J \frac{d\omega_{mec}(t)}{dt}, \quad (7)$$

where $p\omega_{mech}(t) = \omega_{el}(t)$ and M_w is an unknown mechanical load.

III. DESIGN OF A DECOUPLING CONTROL STRATEGY

The present estimator uses the measurements of input voltages, currents and angular velocity of the motor to estimate the "dq" winding inductance, the rotor resistance and amplitude of the linkage flux. The structure of the estimator is described in Fig. 2. This diagram shows how the estimator works. In particular, after having decoupled the system described in (5), the stator resistance R_s and the inductance L_{dq} are estimated through a minimum error variance approach. The estimated values \hat{R}_s and \hat{L}_{dq} are used to estimate the amplitude of the linkage flux ($\hat{\Phi}$). The earliest geometric approaches to

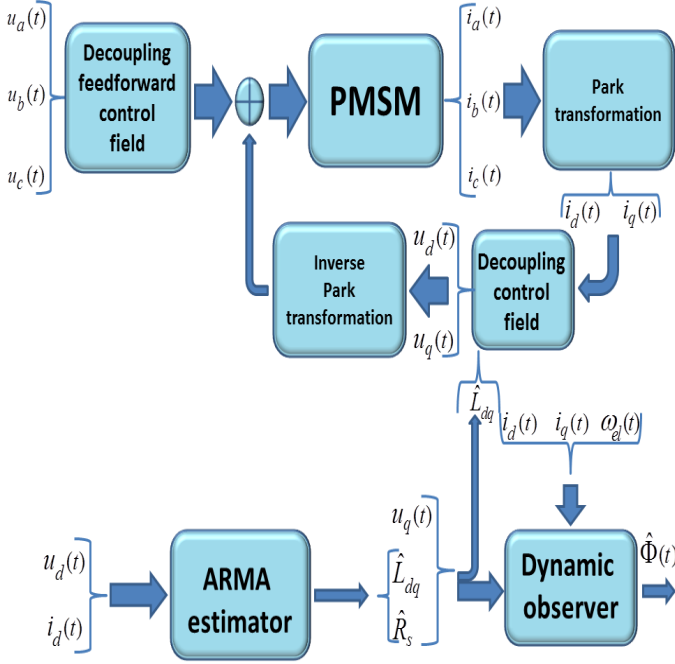


Fig. 2. Conceptual structure of the whole estimator

decoupling control were due to [12] and to [13] and [14]. The following definition taken from [12] recalls the concept of decoupling.

Definition 1: A control law for the dynamic system described by (1), (2) and (3) is *decoupling* with respect to the regulated outputs $i_d(t)$, $i_q(t)$, and $i_o(t)$, if there exist a feedback matrix field $\mathbf{F}(\omega_{el})$ and input partition matrix field $\mathbf{T}(\omega_{el}) = [\mathbf{T}_d, \mathbf{T}_q, \mathbf{T}_o]^T$ of the input voltage vector such that for zero initial conditions, each input $u_{\cdot}(t)$ (with all other inputs, identically zero) only affects the corresponding output $i_d(t)$, $i_q(t)$, or $i_o(t)$. \square

For achieving a decoupled structure of the system described in Eq. (5), a matrix field $\mathbf{F}(\omega_{el})$ is to be calculated such that:

$$(\mathbf{A} + \mathbf{BF}(\omega_{el}))\mathcal{V} \subseteq \mathcal{V}, \quad (8)$$

where $\mathbf{u}(t) = \mathbf{F}(\omega_{el})\mathbf{x}(t)$ is a state feedback with $\mathbf{u}(t) = [u_d(t), u_q(t)]^T$ and $\mathbf{x}(t) = [i_d(t), i_q(t)]^T$,

$$\mathbf{A} = \begin{bmatrix} -\frac{R_s}{L_{dq}} & \omega_{el}(t) \\ -\frac{R_s}{L_{dq}} & \omega_{el}(t) \end{bmatrix}, \quad \mathbf{B} = \begin{bmatrix} \frac{1}{L_{dq}} & 0 \\ 0 & \frac{1}{L_{dq}} \end{bmatrix}, \quad (9)$$

and $\mathcal{V} = \text{im}([0, 1]^T)$ of Eq. (8), according to [12], is a controlled invariant subspace. More explicitly it follows:

$$\mathbf{F}(\omega_{el}) = \begin{bmatrix} F_{11} & F_{12} \\ F_{21} & F_{22} \end{bmatrix}, \text{ and } \begin{bmatrix} u_d(t) \\ u_q(t) \end{bmatrix} = \mathbf{F}(\omega_{el}) \begin{bmatrix} i_d(t) \\ i_q(t) \end{bmatrix},$$

then the decoupling of the dynamics is obtained via the following relationship:

$$\text{im} \left(\begin{bmatrix} -\frac{R_s}{L_{dq}} & \omega_{el}(t) \\ -\frac{R_s}{L_{dq}} & \omega_{el}(t) \end{bmatrix} \right) +$$

$$\text{im} \left(\begin{bmatrix} \frac{1}{L_{dq}} & 0 \\ 0 & \frac{1}{L_{dq}} \end{bmatrix} \begin{bmatrix} F_{11} & F_{12} \\ F_{21} & F_{22} \end{bmatrix} \begin{bmatrix} 0 \\ 1 \end{bmatrix} \right) \subseteq \text{im} \begin{bmatrix} 0 \\ 1 \end{bmatrix}, \quad (10)$$

where parameters F_{11} , F_{12} , F_{21} , and F_{22} are to be calculated in order to guarantee condition (10) and a suitable dynamics for sake of estimation. Condition (10) is guaranteed if:

$$F_{12} = -\omega_{el}(t)L_{dq}. \quad (11)$$

$$\frac{di_d(t)}{dt} = -\frac{R_s}{L_{dq}}i_d(t) + \frac{u_d(t)}{L_{dq}}, \quad (12)$$

Considering now the following output matrix:

$$\mathbf{C} = \begin{bmatrix} 1 & 0 \\ 0 & 1 \end{bmatrix} = \begin{bmatrix} \mathbf{C}_d \\ \mathbf{C}_q \end{bmatrix}. \quad (13)$$

It is to be shown that, if:

$$\mathbf{g}(\omega_{el}) = \begin{bmatrix} \frac{2 \sin(\omega_{el}t)}{3} & \frac{2 \sin(\omega_{el}t-2\pi/3)}{3} & \frac{2 \sin(\omega_{el}t+2\pi/3)}{3} \\ \frac{2 \cos(\omega_{el}t)}{3} & \frac{2 \cos(\omega_{el}t-2\pi/3)}{3} & \frac{2 \cos(\omega_{el}t+2\pi/3)}{3} \\ \frac{1}{3} & \frac{1}{3} & \frac{1}{3} \end{bmatrix}, \quad (14)$$

then there exists a decoupling and stabilizing state feedback matrix field $\mathbf{F}(\omega_{el})$, along with two input partition matrix fields $\mathbf{T}_d(\omega_{el})$, $\mathbf{T}_q(\omega_{el})$, and $\mathbf{T}_c(\omega_{el})$ such that, for the dynamic triples

$$\begin{aligned} & (\mathbf{C}_d, \mathbf{A} + \mathbf{BF}(\omega_{el})), \mathbf{g}(\omega_{el})\mathbf{T}_d, \\ & (\mathbf{C}_q, \mathbf{A} + \mathbf{BF}(\omega_{el})), \mathbf{g}(\omega_{el})\mathbf{T}_q, \end{aligned} \quad (15)$$

it holds the following conditions:

$$\mathcal{R}_d(\omega_{el}) = \min \mathcal{I}(\mathbf{A} + \mathbf{BF}(\omega_{el}), \mathbf{g}(\omega_{el})\mathbf{T}_d(\omega_{el})) \subseteq \mathcal{C}_q \quad \forall \omega_{el}, \quad (16)$$

and

$$\mathbf{C}_d \mathcal{R}_d(\omega_{el}) = \text{im}(\mathbf{C}_d), \quad \forall \omega_{el}. \quad (17)$$

$$\mathcal{R}_q(\omega_{el}) = \min \mathcal{I}(\mathbf{A} + \mathbf{BF}(\omega_{el}), \mathbf{g}(\omega_{el})\mathbf{T}_q(\omega_{el})) \subseteq \mathcal{C}_d \quad \forall \omega_{el}, \quad (18)$$

and

$$\mathbf{C}_q \mathcal{R}_q(\omega_{el}) = \text{im}(\mathbf{C}_q), \quad \forall \omega_{el}. \quad (19)$$

Here,

$$\min \mathcal{I}(\mathbf{A}, \text{im}(\mathbf{BF})) = \sum_{i=0}^{n-1} \mathbf{A}^i \text{im}(\mathbf{B})$$

is a minimum \mathbf{A} -invariant subspace containing $\text{im}(\mathbf{B})$. Moreover, the partition matrix fields $\mathbf{T}_d(\omega_{el})$, $\mathbf{T}_q(\omega_{el})$ and $\mathbf{T}_0(\omega_{el})$ satisfy the following relationships:

$$\begin{aligned} \text{im}(\mathbf{g}(\omega_{el}) \cdot \mathbf{T}_d(\omega_{el})) &= \text{im}(\mathbf{g}(\omega_{el})) \cap \mathcal{R}_d(\omega_{el}), \\ \text{im}(\mathbf{g}(\omega_{el}) \cdot \mathbf{T}_q(\omega_{el})) &= \text{im}(\mathbf{g}(\omega_{el})) \cap \mathcal{R}_q(\omega_{el}). \end{aligned} \quad (20)$$

The stabilizing matrix field $\mathbf{F}(\omega_{el})$ is such that:

$$(\mathbf{A} + \mathbf{BF}(\omega_{el}))\mathcal{R}_d(\omega_{el}) \subseteq \mathcal{R}_d(\omega_{el}), \quad (21)$$

and

$$(\mathbf{A} + \mathbf{BF}(\omega_{el}))\mathcal{R}_q(\omega_{el}) \subseteq \mathcal{R}_q(\omega_{el}). \quad (22)$$

Considering

$$\mathbf{T}(\omega_{el}) = [\mathbf{T}_d(\omega_{el}), \mathbf{T}_q(\omega_{el}), \mathbf{T}_0(\omega_{el}), \mathbf{T}_c(\omega_{el})],$$

where $\mathbf{T}_c(\omega_{el})$ is defined in a complementary fashion and it is straightforward to show that matrix field $\mathbf{T}_c = \mathbf{0}$. In particular, matrix field \mathbf{T}_c represents the complementary matrix field partition to the subspaces of d-coordinate, q-coordinate and 0-coordinate. The system is described using just three variables, therefore partition fields $\mathbf{T}_d(\omega_{el})$ and $\mathbf{T}_q(\omega_{el})$ complete the transformation and thus $\mathbf{T}_c = \mathbf{0}$.

$$\begin{aligned} \text{im}\mathbf{T}(\omega_{el}) &= \text{im}[\mathbf{T}_d(\omega_{el}), \mathbf{T}_q(\omega_{el}), \mathbf{T}_0(\omega_{el})] = \\ &= \text{im}\mathbf{T}_d(\omega_{el}) \oplus \text{im}\mathbf{T}_q(\omega_{el}) \oplus \text{im}\mathbf{T}_0(\omega_{el}). \end{aligned} \quad (23)$$

Considering the output matrix (13) corresponding to d-coordinate, q-coordinate and 0-coordinate, their respective kernels are as follows:

$$\mathcal{C}_d = \text{im} \begin{bmatrix} 0 & 0 \\ 1 & 0 \end{bmatrix}, \quad \mathcal{C}_q = \text{im} \begin{bmatrix} 1 & 0 \\ 0 & 0 \end{bmatrix}. \quad (24)$$

According to definition \mathbf{B} of Eqs. (9) it is straightforward to observe that the following three equations hold $\forall \omega_{el}$:

$$\text{im}(\mathbf{B}) \cap \mathcal{C}_q \neq \mathbf{0}, \quad (25)$$

$$\text{im}(\mathbf{B}) \cap \mathcal{C}_d \neq \mathbf{0}. \quad (26)$$

The following calculations allow to get the required fields for the decoupling of the system:

$$\mathbf{T}_d(\omega_{el}) = (\mathbf{g}(\omega_{el}))^\dagger \cdot \text{im}(\mathbf{B}) \cap \mathcal{C}_q, \quad (27)$$

$$\mathbf{T}_q(\omega_{el}) = (\mathbf{g}(\omega_{el}))^\dagger \cdot \text{im}(\mathbf{B}) \cap \mathcal{C}_d. \quad (28)$$

Field $\mathbf{g}(\omega_{el})$ is a function of ω_{el} without singularities if $\omega_{el}(t) \neq k\pi$ with $k \in \mathbb{N}$, where with $(\mathbf{g}(\omega_{el}))^\dagger$ the pseudo inverse of field $\mathbf{g}(\omega_{el})$ is indicated. Adding all 3 T-Fields together, we get a new field $\mathbf{T}(\omega_{el})$:

$$\mathbf{T}(\omega_{el}) = \mathbf{T}_d(\omega_{el}) + \mathbf{T}_q(\omega_{el}). \quad (29)$$

Field $\mathbf{T}(\omega_{el})$ can be seen as a preselecting field and the following product realises the mechanical decoupling:

$$\mathcal{B} = \text{im}(\mathbf{g}(\omega_{el})\mathbf{T}(\omega_{el})) = \text{im} \begin{bmatrix} 1 & 0 \\ 0 & 1 \end{bmatrix}, \quad (30)$$

in which matrix \mathbf{B} can be seen as a resulting input matrix.

A. A dynamic estimator of Φ

As it is shown in Fig. 2, parameters R_s and L_{dq} can be estimated by using an ARMA identification structure. These two values are needed to estimate flux Φ . If the electrical part of the system "q" and "d" axes is considered, then, assuming that $\omega_{el}(t) \neq 0$, $i_q(t) \neq 0$, and $i_d(t) \neq 0$, the following equation can be considered:

$$\Phi(t) = -\frac{L_{dq} \frac{di_q(t)}{dt} + R_s i_d(t) + L_{dq} \omega_{el}(t) i_q(t) - u_q(t)}{\omega_{el}(t)}. \quad (31)$$

Consider the following dynamic system:

$$\frac{d\hat{\Phi}(t)}{dt} = -\mathcal{K}\hat{\Phi}(t) -$$

$$\mathcal{K} \left(\frac{\hat{L}_{dq} \frac{di_q(t)}{dt} + \hat{R}_s i_d(t)}{\omega_{el}(t)} + \frac{\hat{L}_{dq} \omega_{el}(t) i_q(t) + u_q(t)}{\omega_{el}(t)} \right), \quad (32)$$

where \mathcal{K} is a function to be calculated. Eq. (32) represents the estimators of Φ and \hat{L}_{dq} and \hat{R}_s represent the estimated inductance and resistance respectively by an ARMA procedures in [11]. If the error functions are defined as the differences between the true and the observed values, then:

$$e_\Phi(t) = \Phi(t) - \hat{\Phi}(t), \quad (33)$$

and

$$\frac{de_\Phi(t)}{dt} = \frac{d\Phi(t)}{dt} - \frac{d\hat{\Phi}(t)}{dt}. \quad (34)$$

If the following assumption is given:

$$\left\| \frac{d\Phi(t)}{dt} \right\| \ll \left\| \frac{d\hat{\Phi}(t)}{dt} \right\|, \quad (35)$$

then in Eq. (34), the term $\frac{d\Phi(t)}{dt}$ is negligible. Using Eq. (32), Eq. (34) becomes

$$\begin{aligned} \frac{de_\Phi(t)}{dt} &= \mathcal{K}\hat{\Phi}(t) + \\ &\mathcal{K} \left(\frac{\hat{L}_{dq} \frac{di_q(t)}{dt} + \hat{R}_s i_d(t)}{\omega_{el}(t)} + \frac{\hat{L}_{dq} \omega_{el}(t) i_q(t) + u_q(t)}{\omega_{el}(t)} \right). \end{aligned} \quad (36)$$

Because of Eq. (31), (36) being able to be written as follows:

$$\frac{de_\Phi(t)}{dt} = \mathcal{K}\hat{\Phi}(t) - \mathcal{K}\Phi(t),$$

and considering (33), then:

$$\frac{de_\Phi(t)}{dt} + \mathcal{K}\Phi(t) = 0. \quad (37)$$

\mathcal{K} can be chosen to make Eq. (37) exponentially stable. To guarantee exponential stability, \mathcal{K} must be

$$\mathcal{K} > 0.$$

To guarantee $\left\| \frac{d\Phi(t)}{dt} \right\| \ll \left\| \frac{d\hat{\Phi}(t)}{dt} \right\|$, then $\mathcal{K} \gg 0$. The observer defined in (32) suffers from the presence of the derivative of the measured current. In fact, if measurement noise is present in the measured current, then undesirable spikes are generated by the differentiation. The proposed algorithm must cancel the contribution from the measured current derivative. This is possible by correcting the observed

velocity with a function of the measured current, using a supplementary variable defined as:

$$\eta(t) = \hat{\Phi}(t) + \mathcal{N}(i_q(t)), \quad (38)$$

where $\mathcal{N}(i_q(t))$ is the function to be designed.

Consider

$$\frac{d\eta(t)}{dt} = \frac{d\hat{\Phi}(t)}{dt} + \frac{d\mathcal{N}(i_q(t))}{dt} \quad (39)$$

and let

$$\frac{d\mathcal{N}(i_q(t))}{dt} = \frac{d\mathcal{N}(i_q)}{di_q(t)} \frac{di_q(t)}{dt} = \frac{\mathcal{K}\hat{L}_{dq}}{\omega_{el}(t)} \frac{di_q(t)}{dt}. \quad (40)$$

The purpose of (40) is to cancel the differential contribution from (32). In fact, (38) and (39) yield, respectively:

$$\hat{\Phi}(t) = \eta(t) - \mathcal{N}(i_q(t)), \quad \text{and} \quad (41)$$

$$\frac{d\hat{\Phi}(t)}{dt} = \frac{d\eta(t)}{dt} - \frac{d\mathcal{N}(i_q(t))}{dt}. \quad (42)$$

Substituting (40) in (42) results in:

$$\frac{d\hat{\Phi}(t)}{dt} = \frac{d\eta(t)}{dt} - \frac{\mathcal{K}\hat{L}_{dq}}{\omega_{el}(t)} \frac{di_q(t)}{dt}. \quad (43)$$

Inserting Eq. (43) into Eq. (32), the following expression is obtained:

$$\begin{aligned} \frac{d\eta(t)}{dt} - \frac{\mathcal{K}\hat{L}_{dq}}{\omega_{el}(t)} \frac{di_q(t)}{dt} = & -\mathcal{K}\hat{\Phi}(t) - \\ & \mathcal{K} \left(\frac{\hat{L}_{dq} \frac{di_q(t)}{dt} + \hat{R}_s i_d(t)}{\omega_{el}(t)} + \frac{\hat{L}_{dq} \omega_{el}(t) i_q(t) + u_q(t)}{\omega_{el}(t)} \right), \end{aligned} \quad (44)$$

then:

$$\frac{d\eta(t)}{dt} = -\mathcal{K}\hat{\Phi}(t) - \mathcal{K} \frac{(\hat{R}_s i_d(t) + \hat{L}_{dq} \omega_{el}(t) i_q(t) + u_q(t))}{\omega_{el}(t)}. \quad (45)$$

Letting $\mathcal{N}(i_q(t)) = k_{app} i_q(t)$, where a parameter has been indicated with k_{app} , then from (40) $\Rightarrow \mathcal{K} = \frac{k_{app} \omega_{el}(t)}{\hat{L}_{dq}}$, and Eq. (41) becomes:

$$\hat{\Phi}(t) = \eta(t) - k_{app} i_q(t). \quad (46)$$

Finally, substituting (46) in (45) results in the following equation:

$$\begin{aligned} \frac{d\eta(t)}{dt} = & -\frac{k_{app} \omega_{el}(t)}{\hat{L}_{dq}} (\eta(t) - k_{app} i_q(t)) + \\ & \frac{k_{app}}{\hat{L}_{dq}} (\hat{R}_s i_d(t) + \hat{L}_{dq} \omega_{el}(t) i_q(t) + u_q(t)), \end{aligned}$$

$$\hat{\Phi}(t) = \eta(t) - k_{app} i_q(t). \quad (47)$$

Using the implicit Euler method, the following velocity observer structure is obtained:

$$\begin{aligned} \eta(k) = & \frac{\eta(k-1)}{1 + t_s \frac{k_{app} \omega_{el}(k)}{\hat{L}_{dq}}} + \\ & \frac{t_s \frac{k_{app}^2 \omega_{el}(k) i_q(k)}{\hat{L}_{dq}} + k_{app} \omega_{el}(k) i_q(k) + \frac{t_s \hat{R}_s k_{app} i_d(k)}{\hat{L}_{dq}}}{1 + t_s \frac{k_{app} \omega_{el}(k)}{\hat{L}_{dq}}} i_q(k) + \\ & \frac{t_s \frac{k_{app}}{\hat{L}_{dq}}}{1 + t_s \frac{k_{app} \omega_{el}(k)}{\hat{L}_{dq}}} u_q(k), \\ \hat{\Phi}(k) = & \eta(k) - k_{app} i_q(k), \end{aligned} \quad (48)$$

where t_s is the sampling period.

Remark 1: Assumption (35) states that the dynamics of the approximating observer should be faster than the dynamics of the physical system. This assumption is typical for the design of observers. \square

Remark 2: The estimator of Eq. (48) presents the following limitations: for low velocity of the motor ($\omega_{mec}(t) \ll \omega_{mec_n}(t)$), where $\omega_{mec_n}(t)$ represents the nominal velocity of the motor), the estimation of Φ becomes inaccurate. Because of $\omega_{el}(t)$ dividing the state variable η , the observer described by (48) becomes hyperdynamic. Critical phases of the estimation are the starting and ending of the movement. Another critical phase is represented by a high velocity regime. In fact, it has been proven through simulations, that if $\omega_{mec}(t) \gg \omega_{mec_n}(t)$, then the observer described by (48) becomes hypodynamic. According to the simulation results, within some range of frequency, this hypo-dynamicity can be compensated by a suitable choice of k_{app} . \square

Remark 3: The Implicit Euler method guarantees the finite time convergence of the observer for any choice of k_{app} . Nevertheless, any other method can demonstrate the validity of the presented results. Implicit Euler method is a straightforward one. \square

IV. SIMULATION AND MEASURED RESULTS

The results have been achieved using a special stand with a 58-kW traction PMSM. The stand consists of a PMSM, a tram wheel and a continuous rail. The PMSM is a prototype for low floor trams. The PMSM parameters are: nominal power of 58 kW, nominal torque of 852 Nm, nominal speed of 650 rpm, nominal phase current of 122 A, nominal input voltage of 230 V and the number of poles is 44. The model parameters are: $R = 0.08723$ Ohm, $L_{dq} = L_d = L_q = 0.8$ mH, $\Phi = 0.167$ Wb. The engine has a nominal power of 55 kW, a nominal voltage of 380 V and nominal speed of 589 rpm. Figure 4 shows the estimation measured results of Φ magnet flux. From these figures, the effect of the limit of the procedure discussed in remark 2 is visible at the beginning of the estimation. In particular, this effect is visible in the real measured results. Figure 6 shows a detail of the estimation of the measured

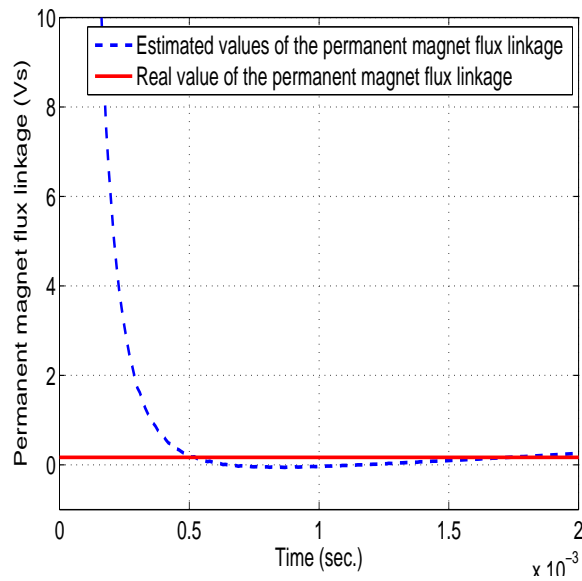


Fig. 3. Simulated results: Estimated and real values of the permanent magnet flux linkage for $k_{app} = 20$

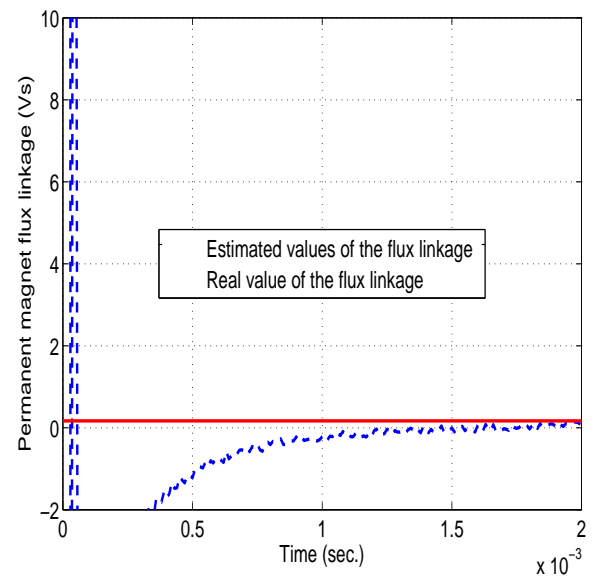


Fig. 5. Detail of the estimation of the measured magnetic flux

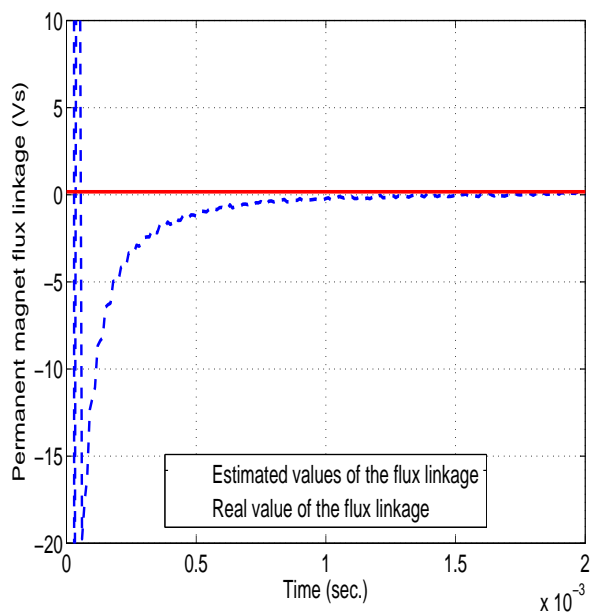


Fig. 4. Measured results

magnetic flux of the motor. In order to recall this effect, it is useful to say that the critical phases of the estimation are the starting and ending of the movement. Another critical phase is represented by a high velocity regime. In fact, it has been proven through simulations and measured results, so that if $\omega_{mec}(t) \gg \omega_{mec_n}(t)$, then the observer described by (48) becomes hypodynamic. Figure 5 shows the angular velocity of the motor. In the present simulations, $t = 0$ corresponds to $\omega_{el}(t) = 0$.

Using a control structure of [15] with PWM frequency equals 100kHz the same results as in [15] are obtained. Figure

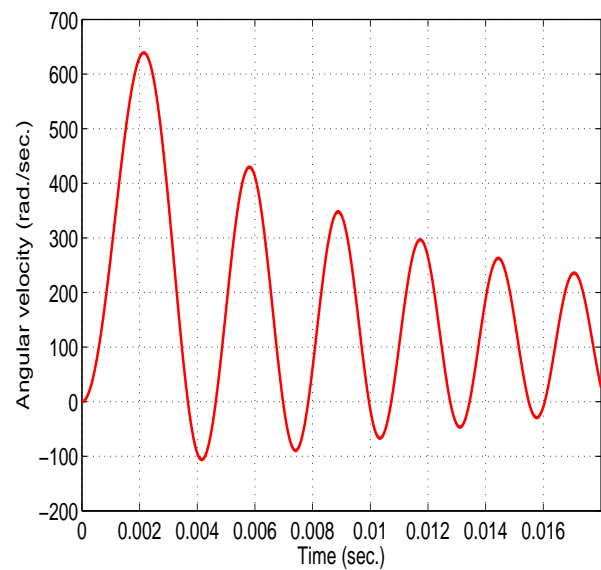


Fig. 6. Angular velocity

7 shows the obtained and desired motor velocity profiles. Figure 8 shows the obtained and desired motor acceleration profiles. From these two results it is possible to remark that the effect of the chopper control is visible which does not allow the tracking to be precise. Figure 9 shows PWM signal sequence with the maximal chopper switching frequency equals 2.5kHz. Figure 10 shows the chopper effect on the input of the motor.

V. CONCLUSIONS AND FUTURE WORK

This paper considers a decoupling dynamic estimator for fully automated parameters identification for three-phase synchronous motors. The proposed strategy uses the geometric

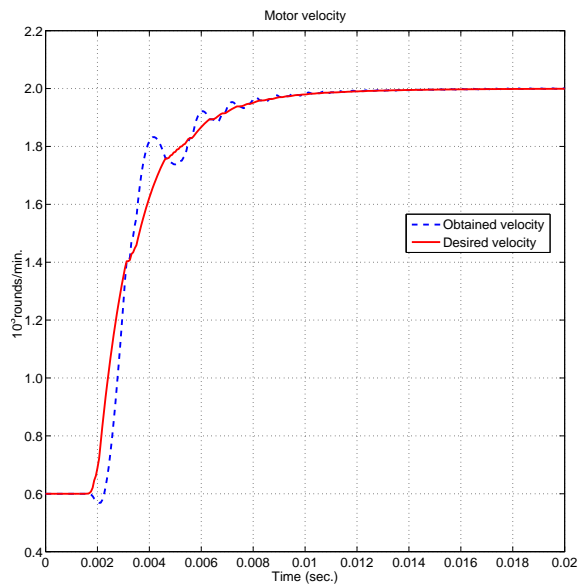


Fig. 7. Profile of the obtained and desired motor velocity using a maximal switching chopper frequency equals 2.5kHz

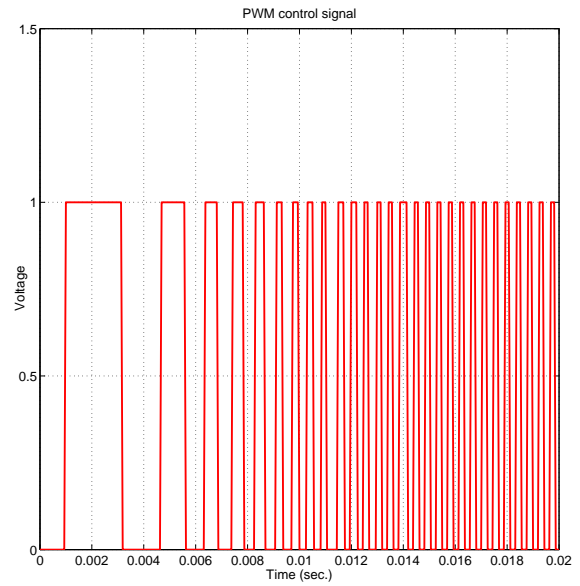


Fig. 9. PWM signal used as a chopper with a maximal switching frequency equals 2.5kHz

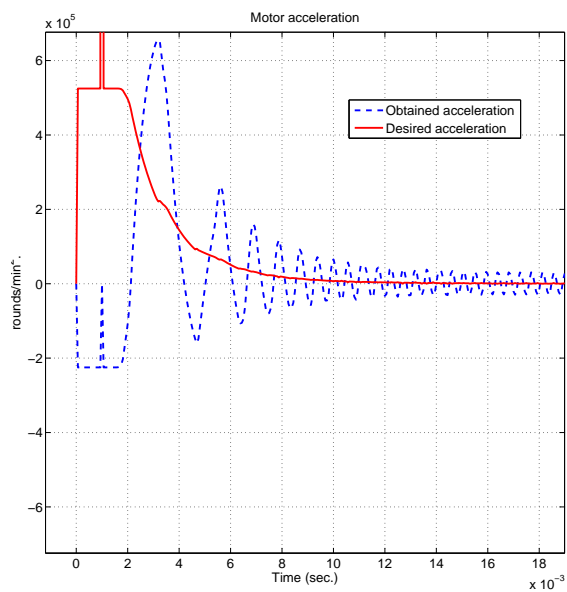


Fig. 8. Profile of the obtained and desired motor acceleration using a maximal switching chopper frequency equals 2.5kHz

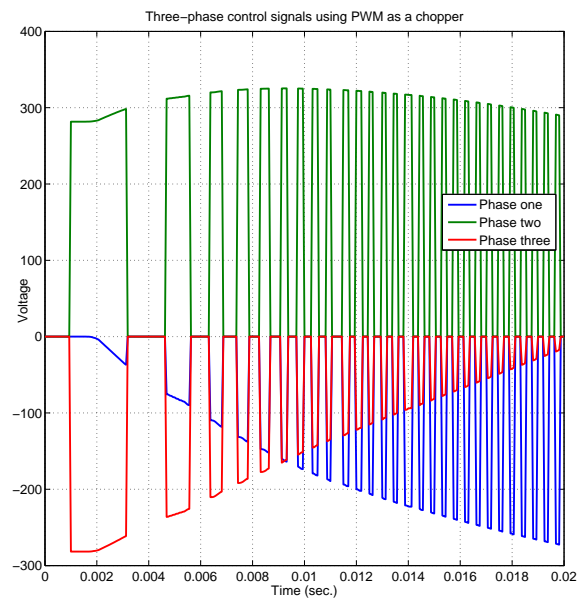


Fig. 10. Three-phase control signals after the chopper controller using a PWM signal with a maximal switching frequency equals 2.5kHz

approach to realised a decoupling of the system. The estimation of the parameters of the motor is simplified through a decoupling. The decoupling is realised using a feedback controller combined with a feedforward one. The feedforward controller is conceived through an input partition matrix. The proposed dynamic estimator is shown to identify the amplitude of the linkage flux using the estimated inductance and resistance. Through simulations and measured results on a synchronous motor used in automotive applications, this paper verifies the effectiveness of the proposed method in identification of PMSM model parameters and discusses the limits of the proposed procedure. Simulation and measured results are reported to validate the proposed strategy. Future work includes the estimation of a mechanical load and the general test of the present algorithm using a real motor.



Paolo Mercorelli received his Master's degree in Electronic Engineering from the University of Florence, Italy, in 1992, and Ph.D. degree in Systems Engineering from the University of Bologna, Italy, in 1998. In 1997, he was a Visiting Researcher for one year in the Department of Mechanical and Environmental Engineering, University of California, Santa Barbara, USA. From 1998 to 2001, he held a postdoctoral position at Asea Brown Boveri, Heidelberg, Germany. Subsequently, from 2002 to 2005, he was a Senior Researcher and Leader of the Control Group, Institute of Automation and Informatics, Wernigerode, Germany, and from 2005 to 2011, he was an Associate Professor of Process Informatics with Ostfalia University of Applied Sciences, Wolfsburg, Germany. In 2011 he was a Visiting Professor at Villanova University, Philadelphia, USA. Since 2012 he has been a Full Professor (Chair) of Control and Drive Systems at the Institute of Product and Process Innovation, Leuphana University of Lueneburg, Germany. His current research interests include mechatronics, automatic control, and signal processing.

REFERENCES

- [1] P. Mercorelli. Invariant subspace for grasping internal forces and non-interacting force-motion control in robotic manipulation. *Kybernetika*, 48(6):1229-1249, 2012.
- [2] P. Mercorelli. Geometric structures using model predictive control for an electromagnetic actuator. *WSEAS TRANSACTIONS on SYSTEMS and CONTROL*, 9:140-149, 2014.
- [3] M.A. Rahman, D.M. Vilathgamuwa, M.N. Uddin, and T. King-Jet. Nonlinear control of interior permanent magnet synchronous motor. *IEEE Transactions on Industry Applications*, 39(2):408-416, 2003.
- [4] P. Mercorelli. A Lyapunov approach for a PI-controller with anti-windup in a permanent magnet synchronous motor using chopper control. *INTERNATIONAL JOURNAL OF MATHEMATICAL MODELS AND METHODS IN APPLIED SCIENCES*, 8(1):44-51, 2014.
- [5] S. Schmidt and P. Mercorelli. Generating energy optimal powertrain force trajectories with dynamic constraints. In *Proceedings of International Conference on Optimization Techniques in Engineering (OTENG'13, WSEAS Conference)*, pages 228-233, Antalya, Turkey, 2013.
- [6] A. Kiltbau and J. Pacas. Appropriate models for the controls of the synchronous reluctance machine. In *Proceedings of the IEEE IAS Annual Meeting*, pages 2289-2295, Pittsburgh, USA, 2002.
- [7] S. Weisgerber, A. Proca, and A. Keyhani. Estimation of permanent magnet motor parameters. In *Proceedings of the IEEE IAS Annual Meeting*, pages 29-34, New Orleans, USA, 1997.
- [8] D.A. Khaburi and M. Shahnazari. Parameters identification of permanent magnet synchronous machine in vector control. In *Proceedings of the 10th European Conference on Power Electronics and Applications, EPE 2003*, Toulouse, 2003.
- [9] P. Mercorelli, K. Lehmann, and S. Liu. On robustness properties in permanent magnet machine control using decoupling controller. In *Proceedings of the 4th IFAC International Symposium on Robust Control Design*, Milan, (Italy), 2003.
- [10] P. Mercorelli. Robust feedback linearization using an adaptive PD regulator for a sensorless control of a throttle valve. *Mechatronics a journal of IFAC*. Elsevier publishing, 19(8):1334-1345, 2009.
- [11] P. Mercorelli. A decoupling dynamic estimator for online parameters identification of permanent magnet three-phase synchronous motors. In *Proceedings of the 16th IFAC Symposium on System Identification, SYSID 2012*, pages 757-762, Brussels, 2012.
- [12] G. Basile and G. Marro. *Controlled and conditioned invariants in linear system theory*. Prentice Hall, New Jersey-USA, 1992.
- [13] W.M. Wonham and A.S. Morse. Decoupling and pole assignment in linear multivariable systems: a geometric approach. *SIAM J. Control*, 8(1):1-18, 1970.
- [14] S.P. Bhattacharyya. Generalized controllability, controlled invariant subspace and parameter invariant control. *SIAM Journal on Algebraic Discrete Methods*, 4(4):529-533, 1983.
- [15] P. Mercorelli. A Lyapunov approach to set the parameters of a pi-controller to minimise velocity oscillations in a permanent magnet synchronous motor using chopper control for electrical vehicles. In *Proceedings of the 2013 International Conference on Systems, Control, Signal Processing and Informatics, (Europment conference)*, pages 151-155, Venice, Italy, 2013.